

## Soil Erosion and Deposition Distribution at Kaoping River Basin under Climate Change

*Kieu Anh Nguyen, Ching-Nuo Chen, Samkele S. Tfwala*

International Master Program in Soil and Water Engineering, National Pingtung University of Science and Technology  
 Department of Civil Engineering, Pingtung University of Science and Technology  
 Pingtung, Taiwan.

### ABSTRACT

In this study we evaluate the impacts of climate change on sediment yield, and soil and deposition distribution at a basin located in southern Taiwan. A numerical model, Physiographic Soil Erosion-Deposition (PSED) Model is verified and applied to simulate the above factors under baseline (1980-1999), and climate change (A1B), for a 24-hour design rainfall for 7 return periods (2, 5, 10, 25, 50, 100 and 200). The model was verified first, by using data from typhoon Morakot in five stations distributed over the basin. Flow hydrographs and sedigraphs were in close agreement for the observed and simulated data. Sediment yield is reduced by 9 % under A1B, 2-year return period and increased by up to 41 % for 200-year return period. Erosion and deposition maps for the basin could be used by the respective personnel for planning and management purposes.

**KEY WORDS:** soil erosion, deposition, climate change, Kaoping watershed.

### INTRODUCTION

Climate change is one of the most significant challenges that all living matters on earth needs to face. The Intergovernmental Panel on Climate Change (IPCC, 2013) reaffirms that the climate is changing in ways that cannot be accounted for by natural variability and that global warming is occurring. It has reported that both land and sea surface temperatures have increased by 0.4 to 0.7°C since the late 19<sup>th</sup> century. Much of the increase in precipitation that has been observed worldwide has been in the form of heavy rainfall. In Taiwan, for example, the frequency of typhoons was one time for every two years before 2000, but it has since increased to an average of 3 to 4 in a year (Tfwala, Wang, and Lin, 2013). This is often accompanied by severe erosion and landslides, especially in Taiwan where on average about 2500 mm falls annually. As such, watershed management is an important component in the control of soil erosion and sediment yield. Understanding soil erosion and deposition, and their distribution is essential for hydraulic installations and for mitigating the consequent impacts. To accomplish such a task, it is necessary to discuss the mechanisms of flood occurrence and soil erosion-deposition caused by significant changes in natural conditions under extreme rainfall within a basin or watershed. In this study, we evaluate the impacts of climate change on erosion and deposition at Kaoping River basin, located in southern Taiwan. A physiographic soil erosion-deposition (PSED) model is used in conjunction with GIS; to simulate soil erosion inundation under 24-hour

design rainfall for baseline (1980-1999) and climate change scenario (2020-2039) A1B for 2, 5, 10, 25, 50, 100 and 200-year return periods. The results from the study will aid government decision-making units related to the development of reference adaptation strategies.

### PHYSIOGRAPHIC SOIL EROSION-DEPOSITION MODEL

To construct the physiographic soil erosion-deposition model in this study, GIS was applied to partition the river basin into computational cells based on the spatial distribution of the physiographic parameters. The computed cells were divided into either land or river cells. The physiographic and hydrological data of each cell were obtained through ArcMap modules and the respective computations were done in two parts as described below:

#### Water Flow Simulation

The purpose of water flow simulation is to calculate the transport of runoff in the watershed. The calculations are based on the continuity equation and discharge formulas. Continuity equation is based on Yang (2000):

$$A_i \frac{\partial h_i}{\partial t} = \sum_k Q_{i,k}(h_i, h_k) + P_{ei}(t) \quad (1)$$

where  $t$  is time;  $A_i$  is the area of the  $i$ -th cell;  $h_i$  is the water depth in the  $i$ -th cell;  $h_k$  is the water stage in the  $k$ -th cell;  $Q_{i,k}$  is the discharge from the the  $k$ -th cell into its neighboring  $i$ -th cell; and  $P_{ei}$  is the effective rainfall volume in the  $i$ -th cell, which is equal to the effective rainfall intensity multiplied by the area of the cell. The effective rainfall volume can be obtained using the following Eqs. 2~3 (Chow, Maidment, and Mays, 1988):

$$P' = (P - 0.2S)^2 / (P + 0.8S) \quad (2)$$

$$S = 2540QCN - 254 \quad (3)$$

where  $P$  is the depth of the total precipitation (mm);  $P'$  is the depth of excess precipitation or direct runoff (mm);  $S$  is less than or equal to the potential maximum retention (mm); and  $CN$  is the curve number. Using finite differentiation, Eq. 1 may be expressed as:

$$h_i^{m+1} = h_i^m + \frac{\left(\sum_k Q_{i,k}^m + P_{ei}^m\right)}{A_i} \cdot \Delta t \quad (4)$$

where  $h_i^{m+1}$  is the water stage in the  $i$ -th cell at time  $m+1$ ;  $h_i^m$  is the water stage in the  $i$ -th cell at time  $m$ ;  $Q_{i,k}$  is the discharge from the  $i$ -th cell into the  $k$ -th cell at time  $m$ ;  $\Delta t$  is time increment between  $t$  and  $t+1$ .

### Soil Erosion Calculations

Using continuity equations for suspended sediment, the sediment transport rate can be determined. For any cell  $i$ , the continuity equations for suspended sediment can be written following the work of Chen et al. (2006):

$$\frac{\partial V_{si}}{\partial t} = \sum_k Q_{SC_{i,k}} + Q_{sei} - Q_{sdi} + R_{DTi} \quad (5)$$

where  $V_{si}$  is the volume of suspended sediment in the  $i$ -th cell ( $= A_i \times D_i \times C_i$ ; where  $C$  is the volumetric concentration of suspended sediment);  $Q_{SC_{i,k}}$  is the transport rate of suspended sediment from the neighboring  $k$ -th cell into the  $i$ -th cell;  $R_{DTi}$  is the rainfall detach rate of the  $i$ -th cell;  $Q_{sei}$  is the entrained sediment volume of bed in the  $i$ -th cell; and  $Q_{sdi}$  is the deposited sediment volume of bed in the  $i$ -th cell.

**Rainfall detach rate.** When flow depth is less than three times the raindrop diameter, rainfall detachment rate in the cell may be expressed as (Mutchler and Young, 1975):

$$R_{DTi} = a \cdot I^b \cdot A_i \quad (6)$$

where  $a$  and  $b$  are variables yet to be determined. Sharma, Gupta, and Foster (1995) suggested that  $b$  be less than 1. Hu et al. found that the range of  $a$  was between 18.36 and 21.72, and that of  $b$  was between 0.81 and 1.29. In this study,  $a = 20$  and  $b = 1$  was selected.

**Entrained sediment and deposition sediment.** According to Itakura and Kishi (1980), the entrained rate of channel bed takes the form:

$$q_{se} = 0.008 \sqrt{sgd} \left[ 0.14 \frac{\rho}{\rho_s} \left( 14 \sqrt{\tau_*} - \frac{0.9}{\sqrt{\tau_*}} \right) - \frac{\omega_s}{\sqrt{sgd}} \right] \quad (7)$$

where  $s = (\rho_s - \rho) / \rho$  is the submerged specific gravity of the sediment;  $\rho_s$  is the density of the sediment;  $\rho$  is the density of the water;  $d$  is the diameter of the sediment;  $\omega_s$  is fall velocity of the sediment; and  $\tau_*$  is the non-dimensional bed shear stress ( $= u_*^2 / sgd$ , where  $u_*$  is the shear velocity).

**Volumetric concentration of suspended sediment.** For the  $i$ -th cell, the explicit finite differentiation representation of Eq. 5 is:

$$C_i^{m+1} = \frac{\left(\sum_k Q_{SC_{i,k}}^m + Q_{sei}^m - Q_{sdi}^m + R_{DTi}^m\right)}{A_i D_i^{m+1}} \cdot \Delta t \quad (8)$$

where  $Q_{SC_{i,k}}$  is the sediment discharge between neighboring  $i$ -th and  $k$ -th cells, which can be determined by the direction of  $Q_{i,k}$  that is the discharge from the  $k$ -th cell into the  $i$ -th cell. If the discharge flows from the  $k$ -th cell into the  $i$ -th cell, then  $Q_{SC_{i,k}} = |Q_{i,k}| \times C_k$ . Conversely, if the discharge flows from the  $i$ -th cell into the  $k$ -th cell, then  $Q_{SC_{i,k}} = -|Q_{i,k}| \times C_i$ .

### THE STUDY AREA

Kaoping River is the largest river in southern Taiwan with a 171 km long main stream and a watershed area of 3257  $km^2$ . The main tributaries of Kaoping River include Laonong, Zhuokou, Ailiao, Wuluo and Qishan rivers (Fig. 1). Due to significant erosion problems, resulting from the river's geographic characteristics and a steep main channel slope, the Kaoping River is famous with serious erosion and sediment deposition among river channels in Taiwan.

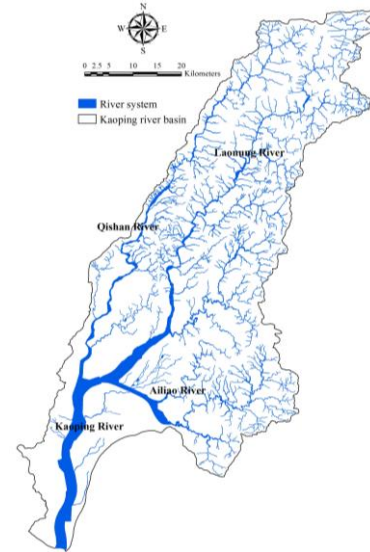


Fig. 1 The study area

ArcGIS™ software (ArcMap® and ArcInfo®) are used to analyse a Digital Elevation Model (DEM) shown in Fig. 2, and to divide the study area into sub-watersheds and computational cells based on topography, landform, vegetation and land use. The entire basin was divided into 17635 irregular grids as illustrated by Fig. 2 using automatic modelling-cell-delimitation method offered by the spatial analyst, hydrologic model and object-oriented programming of ArcMap. All attributes of data fields were calculated to build the necessary database for the PSED model. Further, hydrological data needed for discharge hydrograph and suspended sediment hydrograph simulation were obtained from 28 precipitation gauging stations shown in Fig. 3.

## RESULT AND DISCUSSION

Prior to applying the PSED model, simulation results are compared with observed data to verify the model's reliability in the simulation of runoff and suspended sediment concentration hydrographs.

### Model Verification

The model is verified using observed data of discharge and suspended concentration during Typhoon Morakot in 2009. Five hydrological gauging stations (Shan-Lin, Da-Jin, Liou-Guei, San-Di-Men and Li-lin bridge stations) from the Kaoping river basin were used for validation. The simulated and observed discharge hydrographs for the most downstream (Li-lin bridge station) are shown by Fig. 4.

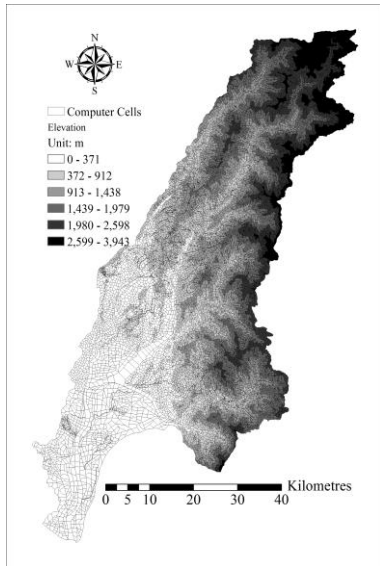


Fig. 2 DEM and computed cells in Kaoping River basin.

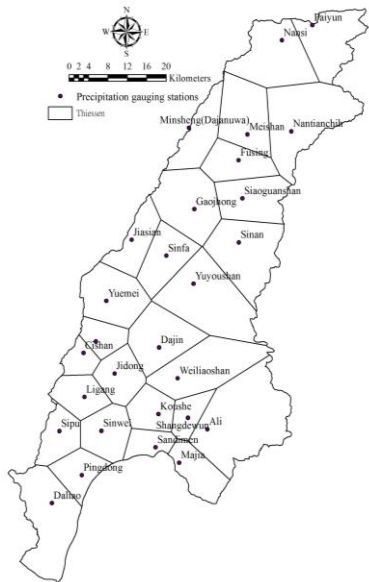


Fig. 3 The precipitation gauge stations and Thiessen polygons.

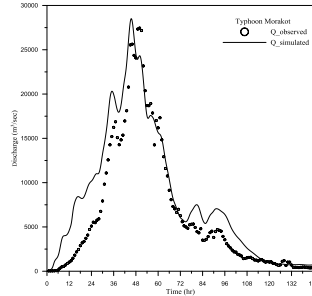


Fig. 4 Comparison of observed and simulated flow discharge for typhoon Morakot. (Li-lin bridge station)

Figure 4 shows the comparison between simulated and observed data. The results show a good fit for the runoff hydrograph. To further validate the PSED model, relationship between observed flow at normal discharge levels and sediment rates obtained from the five river gauging stations is compared with simulated relationships at the same station. The results are shown in Fig. 5.

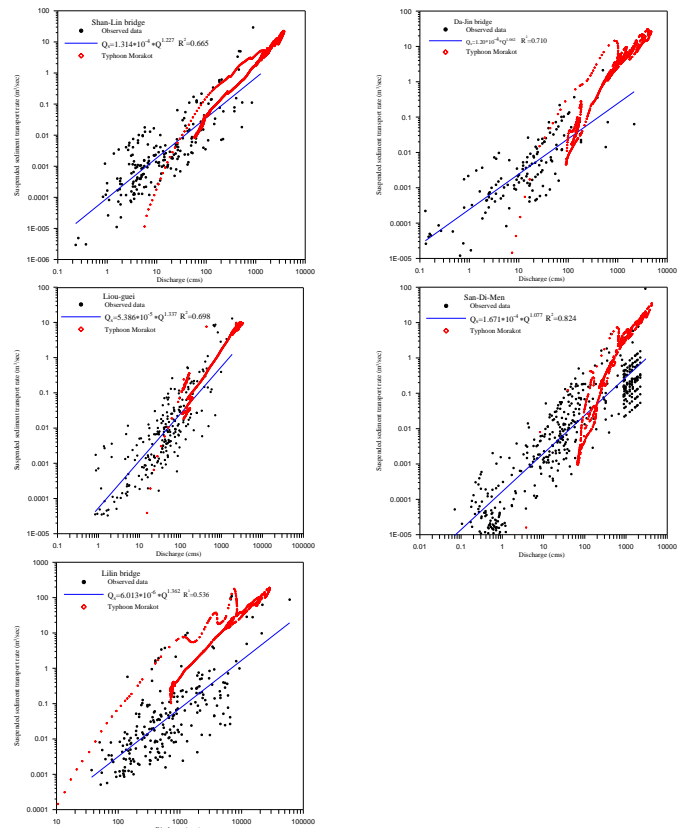


Fig. 5 Comparison of observed and simulated sediment transport rates at the five gauging stations.

### Sediment yields under climate change

Table 1 shows the sediment yield produced (one-day) at Kaoping River basin from the baseline and climate change scenario A1B for the different return periods. The sediment yields are lower under climate change A1B for return periods 2 and 5 year compared with the respective baseline. They are respectively reduced by 9 % and 2 %. Moreover, sediment yield increases more than the baseline from 10 to

200 years return period. This illustrates the possibility of low rainfall amounts in short return periods under climate change and severe rainfall under long return periods is to be expected. Rainfall has been shown to be positively correlated to sediment yield by several researchers (Braun *et al.*, 2000; Kao *et al.*, 2011).

Table 1 Summary of sediment yield under baseline and climate change scenarios

Return period	Baseline	A1B	% Change
2	4,353,244.34	3,950,238.18	-9.26
5	6,203,087.07	6,058,622.59	-2.33
10	7,257,919.91	7,609,300.66	4.84
25	8,454,585.32	9,747,650.38	15.29
50	9,260,978.86	11,448,940.39	23.63
100	10,002,272.50	13,238,706.82	32.36
200	10,685,705.11	15,137,640.18	41.66

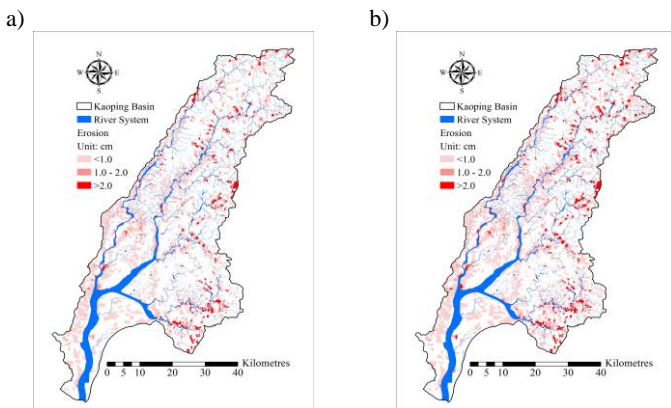


Fig. 6 Erosion distribution under a) baseline and b) A1B 100-yr return period

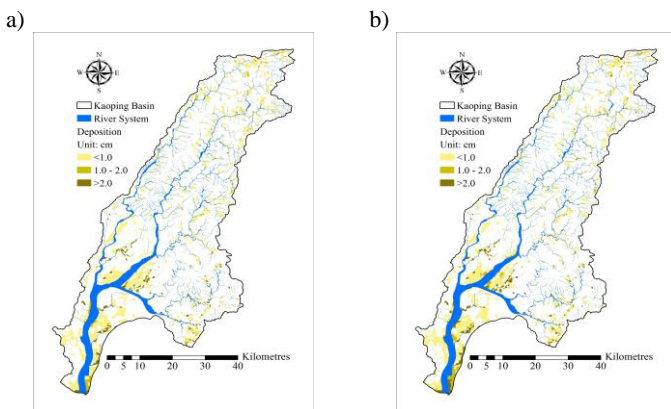


Fig. 7 Deposition distribution under a) baseline and b) A1B 100-yr return period

Figure 6 and 7 shows illustrates the distribution of erosion and deposition within the study area from the baseline (1980-1999) and climate change scenario A1B (2020-2039), respectively, under design rainfall of 24-hour for a 100-year return period. There are visible differences between the baseline and climate change scenarios for both erosion and deposition. Erosion and deposition depths greater than 1

cm increases in both cases. It can also be observed that erosion mainly occurs in areas having steep slopes. For example, greater than 2 cm erosion corresponds to elevation beyond 1000 m, as shown by Fig. 2. This eroded soil is deposited on the low-lying areas (see Fig. 2) as demonstrated in Fig. 7. It is usually in proximity to river systems, and could be an attribute to the huge sediment yield from this basin. Further, it could explain the accelerated agriculture activities observed during reconnaissance visits within the basin. Fertile soils are deposited next to the streams and the combined benefits with nearby water sources are utilised by the land occupants. This could further impact negatively the erosion and deposition rates.

## CONCLUSIONS

Soil erosion is shown to be worsened by climate change at Kaoping River basin. A PSED model was applied to simulate both erosion and deposition under baseline and climate change. The model was verified using data from 5 stations. Simulated and observed results of both flow and sediments were in close agreement, and that justified the adoption of the model. Sediment yield is reduced under climate change scenarios for return periods less than 5, and increased for return periods beyond 5. Sediment yield is increased by up to 41 % under 200-year return periods. Erosion and deposition distribution maps were also produced and these are crucial in identifying areas more sensitive to erosion and could provide the necessary information for better management.

## ACKNOWLEDGEMENTS

This study was supported by the Ministry of Science and Technology (104-2625-M-020-003). The authors gratefully acknowledge the support.

## REFERENCES

- Braun, C., D. R. Hardy, R. S. Bradley, and M. J. Retelle. 2000. Streamflow and Suspended Sediment Transfer to Lake Sophia, Cornwallis Island, Nunavut, Canada, Arctic Antarctic and Alpine Research, 32(4): 456-465. doi: Doi 10.2307/1552395.
- Chow, V. T., D. R. Maidment, and L. W. Mays. 1988. Appli Hydrology. New York: McGraw Hill.
- IPCC. 013. Climate Change 2013: The Physical Science Basis. Tertiary Cambridge, United Kingdom and New York, NY, USA: IPCC.
- Itakura, T. and T. Kishi. 1980. "Open Channel Flow with Suspended Sediments," Journal of Hydraulic Division, 106(8): 1325-1343.
- Kao, S. J., J. C. Huang, T. Y. Lee, C. C. Liu, and D. E. Walling. 2011. "The Changing Rainfall-Runoff Dynamics and Sediment Response of Small Mountainous Rivers in Taiwan under a Warming Climate," Sediment Problems and Sediment Management in Asian River Basins, 349: 114-129.
- Mutchler, C. K. and R. A. Young. 1975. Soil Detachment by Raindrops.
- Sharma, P. P., S. C. Gupta, and G. R. Foster. 1995. "Raindrop-Induced Soil Detachment and Sediment Transport from Interrill Areas," Soil Science Society of America Journal, 59(3): 727-734. doi: 10.2136/sssaj1995.03615995005900030014x.
- Tfwala, S. S., Y. M. Wang, and Y. C. Lin. 2013. "Prediction of Missing Flow Records Using Multilayer Perceptron and Coactive Neurofuzzy Inference System," Scientific World Journal: 584516. doi: 10.1155/2013/584516.
- Yang, C. J. 2000. Study on Construction of a Physiographic Inundation Forecasting System. PhD, Department of Hydraulics and Ocean Engineering, National Cheng-Kung University, Tainan, Taiwan.